

Transition threshold in $\text{GexSb}_{10}\text{Se}_{90-x}$ glasses

Wen-Hou Wei, Liang Fang, Xiang Shen, and Rong-Ping Wang

Citation: *Journal of Applied Physics* **115**, 113510 (2014); doi: 10.1063/1.4869260

View online: <http://dx.doi.org/10.1063/1.4869260>

View Table of Contents: <http://scitation.aip.org/content/aip/journal/jap/115/11?ver=pdfcov>

Published by the [AIP Publishing](#)

Articles you may be interested in

[Structural investigation on \$\text{GexSb}_{10}\text{Se}_{90-x}\$ glasses using x-ray photoelectron spectra](#)

J. Appl. Phys. **115**, 183506 (2014); 10.1063/1.4876258

[Direct hexagonal transition of amorphous \$\(\text{Ge}_2\text{Sb}_2\text{Te}_5\)_{0.9}\text{Se}_{0.1}\$ thin films](#)

Appl. Phys. Lett. **104**, 063505 (2014); 10.1063/1.4865198

[Superstrong nature of covalently bonded glass-forming liquids at select compositions](#)

J. Chem. Phys. **139**, 164511 (2013); 10.1063/1.4826463

[Nonlinear optical studies on nanocolloidal Ga–Sb–Ge–Se chalcogenide glass](#)

J. Appl. Phys. **108**, 073525 (2010); 10.1063/1.3481097

[Third order nonlinearities in Ge - As - Se -based glasses for telecommunications applications](#)

J. Appl. Phys. **96**, 6931 (2004); 10.1063/1.1805182



AIP | Journal of Applied Physics

Journal of Applied Physics is pleased to announce **André Anders** as its new Editor-in-Chief

Transition threshold in $\text{Ge}_x\text{Sb}_{10}\text{Se}_{90-x}$ glasses

Wen-Hou Wei,^{1,2} Liang Fang,^{1,a)} Xiang Shen,³ and Rong-Ping Wang²

¹Department of Applied Physics, Chongqing University, Chongqing 401331, People's Republic of China

²Centre for Ultrahigh Bandwidth Devices for Optical Systems (CUDOS), Laser Physics Centre,

Research School of Physics and Engineering, Australian National University, Canberra ACT 0200, Australia

³Laboratory of Infrared Material and Devices, Advanced Technology Research Institute, Ningbo University, Ningbo 315211, People's Republic of China

(Received 7 January 2014; accepted 11 March 2014; published online 21 March 2014)

$\text{Ge}_x\text{Sb}_{10}\text{Se}_{90-x}$ glasses with Ge content from 7.5 to 32.5 at. % have been prepared by melt-quench technique, and the physical parameters including glass transition temperature (T_g), density (ρ), compactness (C), shear elastic moduli (C_s), compression elastic moduli (C_c), refractive index (n), and optical bandgap (E_g) have been investigated. While all these physical parameters show threshold behavior in the glass with a chemically stoichiometric composition. Raman spectra analysis also indicates that, with increasing Ge content, Se-chains or rings gradually disappear until all Se-atoms are consumed in the glass with a chemically stoichiometric composition. With further increasing Ge content, homopolar Ge-Ge and Sb-Sb bonds are formed and the chemical order in the glasses is violated. The threshold behavior of the physical properties in the $\text{Ge}_x\text{Sb}_{10}\text{Se}_{90-x}$ glasses can be traced to demixing of networks above the chemically stoichiometric composition.

© 2014 AIP Publishing LLC. [<http://dx.doi.org/10.1063/1.4869260>]

I. INTRODUCTION

Chalcogenide glasses (ChGs), which contain the chalcogen elements (S, Se, or Te) as a major constituent covalently bonded with other network forming elements such as Si, Ge, As, and Sb, are attractive candidates for applications in photonics because of their excellent optical properties include high linear and nonlinear refractive indices, high photosensitivity, low transmission losses, and exceptional transmission range (1–16 μm).^{1–3} The applications on the basis of ChGs have been developed including chalcogenide optical fibers and waveguides for telecommunication signals and chemical sensors.⁴ For example, ternary GeAsSe glasses have been well used in various waveguide devices for high-speed all-optical signal processing and a de-multiplexer operating at extreme data rates of 1.28 $\text{Tb} \cdot \text{s}^{-1}$ has recently been demonstrated.^{5–7} Compared with Ge-As-Se, Ge-Sb-Se glasses are less toxic and thus more environmentally acceptable. Higher optical nonlinearity could be expected due to the replacement of As by more metallic Sb. We therefore concentrated on GeSbSe glasses in this paper.

It is well known that the physical properties of the glasses can be tuned via chemical composition since ChGs have a large glass-forming region. It was also suggested that, with changing chemical composition, the physical parameters could exhibit threshold transition that was assigned to segregation of demixing of the heteropolar bonds from the main backbone of the glasses.⁸ However, this has not been examined systematically in Ge-Sb-Se glasses.

In this paper, we prepared numbers of the glasses with fixed Sb concentration of 10 at. % but different Ge concentration changing from 7.5 to 32.5 at. %. Through systematic and comprehensive investigations of the glass structure and physical properties, we aimed at understanding the

evolution of structure and physical properties as a function of glass composition and examining threshold behaviors in $\text{Ge}_x\text{Sb}_{10}\text{Se}_{90-x}$ glasses.

II. EXPERIMENTS

$\text{Ge}_x\text{Sb}_{10}\text{Se}_{90-x}$ bulk glasses were synthesized by the conventional melt quench technique. High purity (5N) Ge, Sb, and Se metals were weighed inside a glove box and loaded into a cleaned and dried quartz ampoule. The loaded ampoule was then sealed under vacuum using an oxygen-hydrogen torch, and introduced into a rocking furnace to melt the contents at a typical temperature around 900–1000 °C for a period not <30 h. The resulting ampoule was subsequently annealed at a temperature 30 °C below the glass transition temperature, and then slowly cooled to room temperature. Following the annealing process, the glasses were sectioned to form discs of 10 mm diameter and approximately 1 mm thick. The discs had their opposite surfaces ground plane parallel and then polished to optical quality. The quality of the glasses was examined using X-ray diffraction (XRD) and infrared (IR) microscopy. XRD patterns indicated the glass structure was amorphous, and IR microscopy revealed the absence of any observable bubbles for all of our glasses.

The glass transition temperature T_g was measured using a differential scanning calorimeter (DSC) (Mettler-Toledo, DSC 1) with a scanning rate of 10 °C min^{-1} . The density (ρ) was measured using a Mettler H20 balance (Mettler-Toledo Ltd, Switzerland) based on the Archimedeian method with a MgO crystal as a reference and acetone as the immersion liquid. Ultrasonic pulse interferometer was employed to measure both shear V_s and compression V_c wave velocities at room temperature with an accuracy of 0.5% at a resonant frequency of 20 MHz. The ultrasonic travel times were systematically corrected to reduce the effect of the bonding layer between the sample and the transducer.⁹ The shear C_s and

^{a)}Electronic mail: lfang@cqu.edu.cn

compression C_c elastic moduli were determined from the measurements of ρ , V_s , and V_c using the formulas $C_s = \rho V_s^2$ and $C_c = \rho V_c^2$, respectively.

Raman spectra were recorded using a T64000 Jobin-Yvon-Horiba micro-Raman spectrometer equipped with a liquid-nitrogen-cooled CCD detector. The 830 nm laser line was used for an excitation source, and the laser power was kept as small as possible to avoid any photo-induced effects. The absorption spectra were recorded using a Varian Cary 5000, UV-Vis-NIR spectrophotometer in the wavelength range from 400 to 1500 nm. The optical gap was estimated at $\alpha \approx 10^3 \text{ cm}^{-1}$. The refractive indices of bulk $\text{Ge}_x\text{Sb}_{10}\text{Se}_{90-x}$ glasses were measured using a Metricon Model 2010 prism coupler with a 1550 nm laser.

III. RESULTS AND DISCUSSION

Raman spectra of $\text{Ge}_x\text{Sb}_{10}\text{Se}_{90-x}$ glasses are shown in Fig. 1. Starting from the glasses with 7.5 at. % Ge content, the spectra are dominated by the bands around 200 cm^{-1} and its shoulder at $\sim 218 \text{ cm}^{-1}$, together with a clear feature at $\sim 256 \text{ cm}^{-1}$. They were attributed to the heteropolar Ge-Se bond vibrations in the corner-sharing and the edge-sharing $\text{GeSe}_{4/2}$ tetrahedra,¹⁰ and Se-Se chain structure,¹¹ respectively. Previously, the vibration of the Sb-Se bond in $\text{SbSe}_{3/2}$ pyramids was confirmed at 195 cm^{-1} .¹² However, we did not observe any clear features that could be ascribed to the vibration of the Sb-Se bonds. This could be due to its weak intensity as well as its overlapping with corner-sharing Ge-Se vibrations.¹³

The intensity of peak at 200 cm^{-1} increases with increasing Ge content, indicating that more Ge-Se corner-sharing $\text{GeSe}_{4/2}$ structure is formed. Its shoulder at 218 cm^{-1} becomes distinguishable with increasing Ge content,

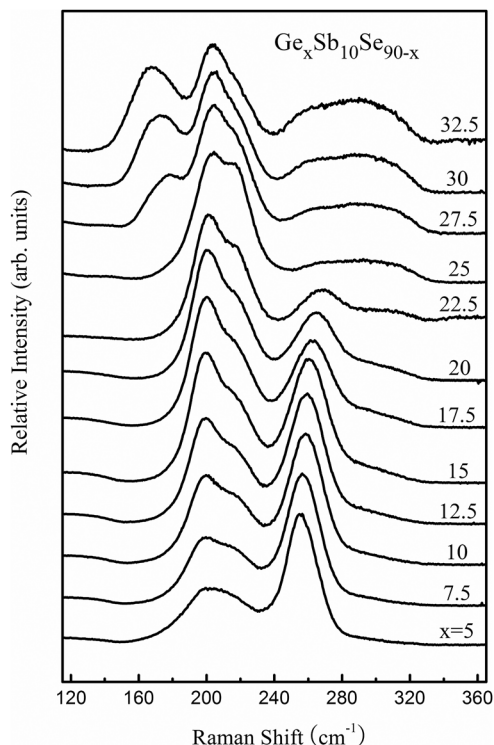


FIG. 1. Raman spectra of $\text{Ge}_x\text{Sb}_{10}\text{Se}_{90-x}$ glasses.

especially in the glasses with a chemically stoichiometric composition containing 25 at. % Ge. However, the shoulder is further smeared out with increasing Ge content from 27.5 at. % to 32.5 at. %. Moreover, a new feature appears at 170 cm^{-1} and gradually shifts to 160 cm^{-1} . The feature could be ascribed to the vibration of homopolar Ge-Ge and Sb-Sb bonds in the Se-poor glasses.^{14,15} Since atomic weight of Sb is heavier than that of Ge, the vibration frequency of Sb-Sb bonds should be less than that of Ge-Ge bonds; therefore, the shift of the peak from 170 to 160 cm^{-1} indicates that, with increasing Ge concentration, Ge-Ge bonds are formed before Sb-Sb bonds.

Another feature at 256 cm^{-1} corresponding to Se-chain structure becomes weak in its intensity and slightly shifts to high wavenumber with increasing Ge content, and this feature completely disappears at the stoichiometric glasses, which could be attributed to a decrease in the concentration of Se-Se units. In addition, with further increasing Ge content, the broad band at a region from 230 to 330 cm^{-1} was assigned to the stretching vibration of Ge-Ge bonds in modified $\text{Se}_3\text{Ge}-(\text{GeSe}_2)_{0.1}-\text{GeSe}_3$ and in $\text{Ge-Ge}_m\text{Se}_{4-m}$ ($m = 1, 2, 3, 4$) units¹⁶ due to the shortage of Se in the glasses.

Overall, the present Raman spectra clearly show a transition behavior in the stoichiometric glasses, the disappearance of 256 cm^{-1} peak at the stoichiometric composition is a symbol of complete consuming of Se-Se units, and the appearance of 160 – 170 cm^{-1} band with increasing Ge content reflects the formation of the homopolar Ge-Ge and Sb-Sb bonds.

It is well established that glass transition temperature (T_g) depends on the glass network connectivity and average bond energy.^{17,18} As shown in Fig. 2, it is clear that T_g increases progressively with increasing Ge content in the Se-rich range until it reaches a maximum at stoichiometric composition, i.e., $\text{Ge}_{25}\text{Sb}_{10}\text{Se}_{65}$, and then decreases with further increase of Ge content. On the one hand, from the structural viewpoint, Raman spectra in Fig. 1 indicated that, for the glasses with low Ge content, Se chains along with Se rings dominate glass structures. With increasing Ge content, different molecular units including $\text{SbSe}_{3/2}$ pyramids and $\text{GeSe}_{4/2}$ tetrahedra will cross-link together, leading to an increase in T_g until all Se

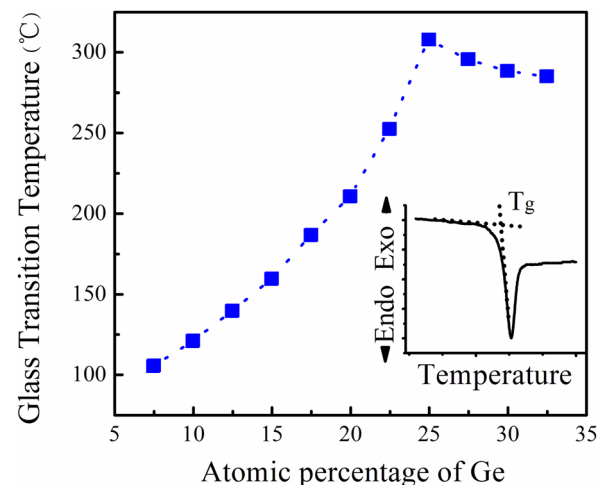


FIG. 2. Glass transition temperatures of $\text{Ge}_x\text{Sb}_{10}\text{Se}_{90-x}$ glasses. The inset shows the definition of glass transition temperature.

atoms are consumed by Ge and Sb. Further addition of Ge content leads to the formation of the homopolar Ge-Ge and Sb-Sb bonds in order to compensate the deficiency of Se. Moreover, previous results indicated that the homopolar Ge-Ge and Sb-Sb bonds could destroy network connectivity due to demixing, leading to a decrease of T_g for the glasses with high Ge content above the chemical threshold.

On the other hand, the bond energies of Ge-Se, Sb-Se, Se-Se, Ge-Ge, and Sb-Sb bonds are 56, 51, 49, 45, and 30 KCal · mol⁻¹, respectively.¹⁹ From an energy point of view, the formation of heteropolar bonds is favoured over the formation of homopolar bonds. The progressive increase in Ge content in Se-rich glasses results in an increase in average bond energy of the system until the highest bond energy appears at the stoichiometric composition. However, for the Se-poor glasses, with the decrease of Se content, Ge-Se and Sb-Se bonds correspondingly decrease; meanwhile, more Ge-Ge and Sb-Sb structural units can be formed, leading to a decrease of T_g due to lower average bond energy in Ge-Sb-Se glasses.

The compactness coefficient C reflects the normalized change of the mean atomic volume due to chemical interactions of the elements forming the network of a given solid. Its correlation with the density can be expressed as,²⁰

$$C = \rho \left(\sum_i \frac{A_i x_i}{\rho_i} - \sum_i \frac{A_i x_i}{\rho} \right) / \sum_i A_i x_i, \quad (1)$$

where ρ , A_i , x_i , and ρ_i represent glass density, atomic weight, atomic fraction, and density of the i th element of the glass, respectively. Figure 3 shows the density and the compactness of Ge_xSb₁₀Se_{90-x} glasses. Obviously, both the density and the compactness have a minimum at 25 at. % of Ge concentration. Again, the transition threshold occurs at the chemically stoichiometric glass. Noteworthy is that, in Ge_xSb₁₀Se_{90-x} glasses, since Ge is lighter than Se, the replace of Se by Ge should lead to the decrease of the density if the glass structure was kept same. Therefore, the threshold behavior observed here can be attributed to that the covalent glass network undergoes a structural rearrangement from being less compact (Ge concentration < 25 at. %) to being more compact (Ge concentration > 25 at. %).

Figure 4 shows the shear and compression elastic moduli for Ge_xSb₁₀Se_{90-x} glasses. Both the shear and the

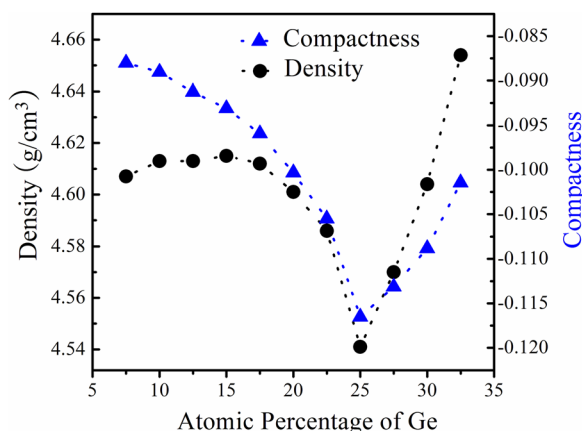


FIG. 3. Density and compactness of Ge_xSb₁₀Se_{90-x} glasses.

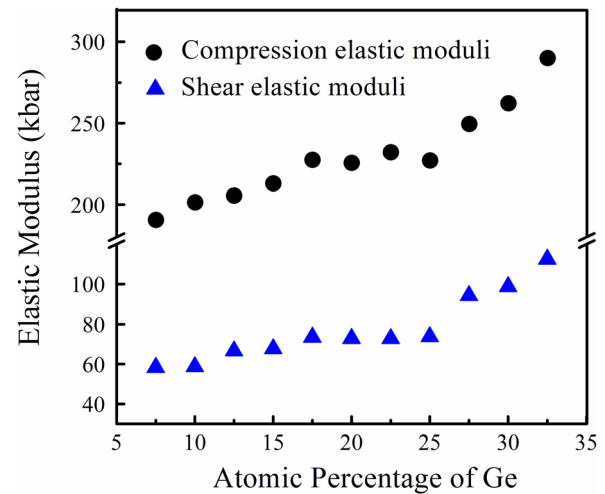


FIG. 4. Shear and compressional elastic moduli in Ge_xSb₁₀Se_{90-x} glasses.

compression elastic moduli increase with increasing Ge content, especially, a steep increase in elastic moduli above the stoichiometric composition. For the glasses with low Ge content up to the stoichiometric composition, the density decreases but the elastic moduli increase as Ge content increases, that is due to the fact that glass structure gradually changes from Se-chain or -ring dominated to SbSe_{3/2} pyramids and GeSe_{4/2} tetrahedra cross-linked. Such low-dimensional Se-chain or -ring structural units are likely to weaken the network structure, while three-dimensional SbSe_{3/2} pyramids and GeSe_{4/2} tetrahedra strengthen the network. Above the chemically stoichiometric composition, more three-dimensional structural units and higher density contribute to the steep increase in the shear and compression elastic moduli of the glasses.

Figure 5 shows refractive index and optical bandgap of Ge_xSb₁₀Se_{90-x} glasses as a function of chemical composition. It is evident that the refractive index decreases before it reaches a minimum at 25 at. % Ge content, and then increases with further increase in Ge concentration. On the contrary, the optical bandgap increases until a maximum appears at 25 at. % Ge content, then decreases with further increasing Ge content. Again, the threshold behaviors occur at the chemically stoichiometric glass. In addition, the correlation of the bandgap and refractive index is in excellent

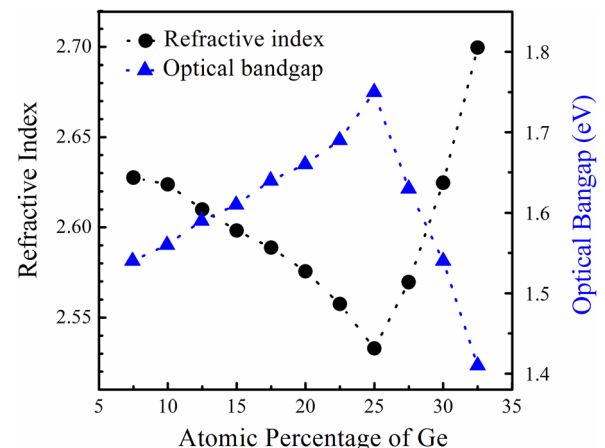


FIG. 5. Refractive index and optical bandgap of Ge_xSb₁₀Se_{90-x} glasses.

agreement with the Moss rule²¹ where the value of $E_g \cdot n^4$ should be a constant, in our case the value is 73 ± 0.5 eV for $\text{Ge}_x\text{Sb}_{10}\text{Se}_{1-x}$ glasses.

In chalcogenide glasses, the existence of defective units like Se-Se, Ge-Ge, and Sb-Sb bonds forms band-tails,²² and thus the increase of the defects will extend band-tails into the gap and narrow the optical band gap. This is reflected in Fig. 5 where E_g increases until the chemical stoichiometric composition is reached, and then starts to decrease with increasing Ge content. The decrease of Se-Se bonds in the glasses with Ge content below 25 at. %, and the increase of Ge-Ge and Sb-Sb bonds in the glasses with Ge content above 25 at. % are the main reason why we observe a maximum E_g at the chemically stoichiometric glass, where all Se atoms are consumed by Ge and Sb atoms and thus “more ordered” structure is formed in chemically stoichiometric glass with a minimum bandtail and a maximum E_g .

The present paper clearly shows that all the properties exhibit threshold behavior at the chemically stoichiometric glasses. Regarding the microscopic nature of the transitions at a molecular level, the stochastic agglomeration theory suggested that glass transition temperature (T_g) is a good measure of global connectivity in glass network.²³ Boolchand *et al.*²⁴ investigated the threshold behavior in T_g and suggested that, above the threshold, phase separation can occur in the nano- or micrometer scale, i.e., the Ge-Sb-Se glass network consists of demixed structural units of $\text{GeSe}_{4/2}$ and $\text{SbSe}_{3/2}$. The heteropolar bonds segregated from the main backbone, destroying the connectivity of the glass network and reducing T_g . The extreme value of T_g observed at the chemical stoichiometric composition is strikingly similar to the threshold behavior that has been observed in this paper. This suggests that the threshold behavior of the physical properties in the Ge-Sb-Se system can be traced to “demixing” of networks above the chemical threshold.

IV. CONCLUSIONS

We have prepared a series of $\text{Ge}_x\text{Sb}_{10}\text{Se}_{90-x}$ glasses and systematically investigated their structural and physical properties like glass transition temperature, density, compactness, elastic moduli, refractive index, and optical bandgap. While Raman spectra of the glasses show that, with increasing Ge content, Se-chains or rings gradually disappear until all Se-atoms are consumed in the glass with a chemically stoichiometric composition, and homopolar Ge-Ge and Sb-Sb bonds are formed with further increasing Ge content. The formation of the homopolar bonds is considered to play an important role in “demixing” of networks above the chemical threshold, leading to the threshold behavior in the glasses.

ACKNOWLEDGMENTS

This research was supported by the Australian Research Council (ARC) Centre of Excellence for Ultrahigh Bandwidth Devices for Optical System (project CE110001018), the ARC Discovery programs (project DP110102753), the National Program on Key Basic Research Project (973 Program)

(Grant No. 2012CB722703), and the Natural Science Foundation of China (Grant No. 61377061).

- ¹J. A. Savage, P. J. Webber, and A. M. Pitt, “Assessment of Ge-Sb-Se glasses as 8 to 12 μm infra-red optical-materials,” *J. Mater. Sci.* **13**, 859–864 (1978).
- ²A. M. Andriesh, “Properties of chalcogenide glasses for optical waveguides,” *J. Non-Cryst. Solids* **77**, 1219–1228 (1985).
- ³Z. Cimprl and F. Kosek, “Utilization of chalcogenide glasses in infrared optics,” *J. Non-Cryst. Solids* **90**, 577–579 (1987).
- ⁴P. Lucas, M. R. Riley, C. Boussard-Pledel, and B. Bureau, “Advances in chalcogenide fiber evanescent wave biochemical sensing,” *Anal. Biochem.* **351**, 1–10 (2006).
- ⁵B. J. Eggleton, B. Luther-Davies, and K. Richardson, “Chalcogenide photonics,” *Nat. Photonics* **5**, 141–148 (2011).
- ⁶X. Gai, T. Han, A. Prasad, S. Madden, D. Y. Choi, R. P. Wang, D. Bulla, and B. Luther-Davies, “Progress in optical waveguides fabricated from chalcogenide glasses,” *Opt. Express* **18**, 26635–26646 (2010).
- ⁷T. D. Vo, H. Hu, M. Galili, E. Palushani, J. Xu, L. K. Oxenlowe, S. J. Madden, D. Y. Choi, D. A. P. Bulla, M. D. Pelusi, J. Schroder, B. Luther-Davies, and B. J. Eggleton, “Photonic chip based transmitter optimization and receiver demultiplexing of a 1.28 Tbit/s OTDM signal,” *Opt. Express* **18**, 17252–17261 (2010).
- ⁸P. Boolchand, D. G. Georgiev, T. Qu, F. Wang, L. C. Cai, and S. Chakravarty, “Nanoscale phase separation effects near $r=2.4$ and 2.67, and rigidity transitions in chalcogenide glasses,” *C. R. Chim.* **5**, 713–724 (2002).
- ⁹R. P. Wang, A. Smith, B. Luther-Davies, H. Kokkonen, and I. Jackson, “Observation of two elastic thresholds in $\text{Ge}_x\text{As}_y\text{Se}_{100-x-y}$ glasses,” *J. Appl. Phys.* **105**, 056109 (2009).
- ¹⁰K. Jackson, A. Briley, S. Grossman, D. V. Porezag, and M. R. Pederson, “Raman-active modes of a- GeSe_2 and a- GeS_2 : A first-principles study,” *Phys. Rev. B* **60**, R14985–R14989 (1999).
- ¹¹Y. Wang, O. Matsuda, K. Inoue, O. Yamamuro, T. Matsuo, and K. Murase, “A Raman scattering investigation of the structure of glassy and liquid $\text{Ge}_x\text{Se}_{1-x}$,” *J. Non-Cryst. Solids* **232**, 702–707 (1998).
- ¹²J. Holubova, Z. Cernosek, and E. Cernoskova, “ $\text{Sb}_x\text{Se}_{100-x}$ system ($0 \leq x \leq 8$) studied by DSC and Raman spectroscopy,” *Optoelectron Adv. Mater.* **1**, 663–666 (2007).
- ¹³Z. G. Ivanova, V. Pamukchieva, and M. Vlcek, “On the structural phase transformations in $\text{Ge}_x\text{Sb}_{40-x}\text{Se}_{60}$ glasses,” *J. Non-Cryst. Solids* **293**, 580–585 (2001).
- ¹⁴S. Bhosle, K. Gunasekera, P. Boolchand, and M. Micoulaut, “Melt homogenization and self-organization in chalcogenides-Part II,” *Int. J. Appl. Glass Sci.* **3**, 205–220 (2012).
- ¹⁵A. Prasad, C. J. Zha, R. P. Wang, A. Smith, S. Madden, and B. Luther-Davies, “Properties of $\text{Ge}_x\text{As}_y\text{Se}_{100-x-y}$ glasses for all-optical signal processing,” *Opt. Express* **16**, 2804–2815 (2008).
- ¹⁶O. Uemura, Y. Kameda, S. Kokai, and T. Satow, “Thermally induced crystallization of amorphous $\text{Ge}_{0.4}\text{Se}_{0.6}$,” *J. Non-Cryst. Solids* **117**, 219–221 (1990).
- ¹⁷S. Mahadevan and A. Giridhar, “Floppy to rigid transition and chemical ordering in Ge-Sb(As)-Se glasses,” *J. Non-Cryst. Solids* **143**, 52–58 (1992).
- ¹⁸L. Tichy and H. Ticha, “Covalent bond approach to the glass-transition temperature of chalcogenide glasses,” *J. Non-Cryst. Solids* **189**, 141–146 (1995).
- ¹⁹J. Bicerano and S. R. Ovshinsky, “Chemical bond approach to the structures of chalcogenide glasses with reversible switching properties,” *J. Non-Cryst. Solids* **74**, 75–84 (1985).
- ²⁰M. Vlcek and M. Frumar, “Model of photoinduced changes of optical-properties in amorphous layers and glasses of Ge-Sb-S, Ge-S, As-S and As-Se systems,” *J. Non-Cryst. Solids* **97**(8), 1223–1226 (1987).
- ²¹T. S. Moss, “Relations between the refractive-index and energy-gap of semiconductors,” *Phys. Status Solidi B* **131**, 415–427 (1985).
- ²²K. Hachiya, “Electronic structure of the wrong-bond states in amorphous germanium sulphides,” *J. Non-Cryst. Solids* **321**, 217–224 (2003).
- ²³M. Micoulaut and G. G. Naumis, “Glass transition temperature variation, cross-linking and structure in network glasses: A stochastic approach,” *Europhys. Lett.* **47**, 568–574 (1999).
- ²⁴P. Boolchand, P. Chen, and U. Vempati, “Intermediate phases, structural variance and network demixing in chalcogenides: The unusual case of group V sulfides,” *J. Non-Cryst. Solids* **355**, 1773–1785 (2009).